Journal of Solid State Chemistry 184 (2011) 2439–2445

Contents lists available at ScienceDirect

Journal of Solid State Chemistry

journal homepage: www.elsevier.com/locate/jssc

Methotrexate intercalated ZnAl-layered double hydroxide

Manjusha Chakraborty [a], Sudip Dasgupta [a], Chidambaram Soundrapandian [a], Jui Chakraborty [a,*], Swapankumar Ghosh [b,**], Manoj K. Mitra [c], Debabrata Basu [a]

[a] Central Glass & Ceramic Research Institute, CSIR, 196 Raja S.C. Mullick Road, Kolkata 700032, India
[b] National Institute for Interdisciplinary Science & Technology (NIIST), CSIR, Trivandrum 695019, India
[c] Department of Metallurgical and Materials Engineering, Jadavpur University, Kolkata 700032, India

ARTICLE INFO

Article history:
Received 7 April 2011
Received in revised form
5 July 2011
Accepted 11 July 2011
Available online 19 July 2011

Keywords:
Layered double hydroxides
Methotrexate
Intercalation
Hybrids
Release kinetics

ABSTRACT

The anticancerous drug methotrexate (MTX) has been intercalated into an ZnAl-layered double hydroxide (LDH) using an anion exchange technique to produce LDH–MTX hybrids having particle sizes in the range of 100–300 nm. X-ray diffraction studies revealed increases in the basal spacings of ZnAl-LDH–MTX hybrid on MTX intercalation. This was corroborated by the transmission electron micrographs, which showed an increase in average interlayer spacing from 8.9 Å in pristine LDH to 21.3 Å in LDH–MTX hybrid. Thermogravimetric analyses showed an increase in the decomposition temperature for the MTX molecule in the LDH–MTX hybrid indicating enhanced thermal stability of the drug molecule in the LDH nanovehicle. The cumulative release profile of MTX from ZnAl-LDH–MTX hybrids in phosphate buffer saline (PBS) at pH 7.4 was successfully sustained for 48 h following Rigter-Peppas model release kinetics via diffusion.

1. Introduction

Layered double hydroxides (LDHs), considered to be promising new generation materials, comprise two-dimensional layers with structure similar to that of mineral brucite, $Mg(OH)_2$ [1]. LDHs have many properties, which make them attractive for real applications, these include nanomedicine [1,2], adsorbents [2,3], catalyst supports [2,4,5], controlled release of anions [6–8] and antacids [9]. The high versatility, easily tailored properties and low cost of LDHs make them promising candidates as host materials for the transport and delivery of gene [10] or drug due to their low toxicity, pH dependent solubility and enhanced cellular uptake behaviour [11]. Cancer cells that have high level resistance to radiotherapy, notably osteosarcoma, chemotherapy is the only alternative [12]. High dose methotrexate (MTX), a folic acid antagonist, with leucovorin rescue is the drug of choice used in the therapy of this malignancy [13]. Intensive investigations in the area of targeted drug delivery to combat cancer has prompted the use of LDHs [14,15], that have a cationic framework formed by the isomorphous substitution of M^{2+} (where M is Mg, Ca, Zn Fe, Cu, Mn, etc.) ions, with M^{3+} (where M is Al, Fe, Cr, Co, etc.) ions in a structure of $M^{2+}(OH)_2$ [2]. As a result, LDHs possess invariably high anion exchange capacities with relatively weak interlayer bonding. The interlayer anions can be ion-exchanged with an equivalent amount of MTX molecules. The cationic layers of LDHs act as safe reservoir for the MTX and other biofunctional molecules [16]. MTX intercalated LDHs are reported to have high resistance against enzymatic degradation during its transport to specific cells or tissues [16,17]. The role of MTX intercalated MgAl-LDH has previously been reported in preventing proliferation of cancerous cells and tissues [10,18]. The efficacy of the MgAl-LDH–MTX hybrid is found to be nearly 5000 times greater in inhibiting cell proliferation in osteocarsoma cell lines as compared to the free MTX drug molecule [10,14,18]. MgAl-LDH materials have also been reported as effective carriers of anticancerous agents such as folic acid [19]. The ion exchangeability and biodegradability of LDHs in acidic media in the vicinity of cancerous cells give rise to controlled release of intercalated molecules. Among a range of biocompatible LDHs being studied as effective drug delivery systems, the effectiveness and importance of ZnAl-LDHs as a carrier for controlled release of drug molecules has not yet been fully addressed. In its ionic form, zinc plays a vital role in the human body, for example, it protects from DNA-damage [20], useful in cancer therapy [21] and controls the activities of more than 200 enzymes [22]. LDHs have been generally synthesized by either coprecipitation of precursor nitrate solution using NaOH [23], anion exchange methods [24] or sol–gel methods [25].

Hou et al. studied the effectiveness of ZnAl-LDH as a carrier for 5-fluorocytocine [26]. However, to the best of our knowledge, there is no report in the published literature on the study of

* Corresponding author. Fax: +91 33 24730957.
** Corresponding author.
E-mail addresses: jui@cgcri.res.in (J. Chakraborty), swapankumar.ghosh2@mail.dcu.ie (S. Ghosh).

0022-4596/$ - see front matter © 2011 Elsevier Inc. All rights reserved.
doi:10.1016/j.jssc.2011.07.015

incorporation of MTX anionic drug in a ZnAl-LDH carrier. The Chemical structure of MTX is similar to that of dihydrofolic acid (Fig. S1 in Supplementary material). Herein, we report synthesis of a ZnAl-LDH nanocarrier by a simple coprecipitation method. MTX is intercalated into the LDH interlayers by an anion exchange technique. The LDH–MTX composite was fully characterized using powder X-ray diffraction (XRD), transmission electron microscopy (TEM), field emission scanning electron microscopy (FESEM), thermogravimetric analyses (TG), Fourier transform infrared spectroscopy (FTIR) and particle size analysis. MTX loading in the formulation was confirmed by carbon hydrogen nitrogen (CHN) elemental analyses and thermal analyses. The release behaviour of MTX from the hybrid material was studied using high performance liquid chromatography (HPLC). All the results are discussed and correlated, which shows the potential of ZnAl-LDH in controlled drug delivery.

2. Experimental procedure

2.1. Materials

Zinc nitrate hexahydrate [$Zn(NO_3)_2.6H_2O$], aluminium nitrate nonahydrate [$Al(NO_3)_3.9H_2O$], sodium hydroxide and ammonium hydroxide (25%) were purchased from Sigma Aldrich and Sun laboratory (Bangalore, India) supplied methotrexate (MTX powder form, calibration standard drug). Deionised and decarbonated ultrapure water (Millipore, specific resistivity 18 MΩ) was used in all preparations and the chemicals utilized in this study were used as received without further purification.

2.2. Synthesis of ZnAl–MTX LDH hybrid material

20 mmol $Zn(NO_3)_2.6H_2O$ (Sigma Aldrich) and 10 mmol $Al(NO_3)_3.9H_2O$ (Sigma Aldrich) were dissolved in 250 mL water. To this mixed metal precursor solution, 0.01 M NaOH (Sigma Aldrich) was added drop wise until pH=8 in nitrogen atmosphere, with strong magnetic stirring. The stirring was continued for further 24 h. The appearance of a white gelatinous precipitate indicated the formation of ZnAl-LDH. The precipitate was collected by centrifugation and washed repeatedly by redispersing it in water followed by centrifugation to remove excess nitrate anions. The washed LDH precipitate was lyophilized to get dry ZnAl-LDH nanopowder.

Subsequently, 1.2 g MTX was dissolved in 50 mL water of pH 7.5 (pH was raised by the addition of 25% NH_4OH) and the solution was added to 100 mL aqueous suspension containing 1 g LDH. The pH of the LDH–MTX mixture was raised to ~8.5 by drop wise addition of 0.01 M NaOH. The reaction mixture was agitated for 72 h in nitrogen atmosphere. The product, ZnAl-LDH–MTX, was centrifuged, washed with deionized water thoroughly and lyophilized (EYEL4, FDU2200, Japan).

2.3. Preparation of samples for HPLC analysis

10 mg of ZnAl-LDH–MTX formulation was dispersed in 30 mL of PBS of pH 7.4. An aliquot of 1 mL was taken for analysis and was replenished to keep the final volume constant. It was filtered through a 0.2 μm membrane filter paper. 20 μL aliquots of the filtered solution were analysed by HPLC using Tris buffer (0.1 M KH_2PO_4 and 0.01 M Tris–HCl), acetonitrile and methanol in 80:10:10 ratio (v/v) as eluent.

2.4. Characterization

Powder X-ray diffraction (XRD) patterns were obtained for ZnAl-LDH and ZnAl-LDH–MTX powders with X'Pert Pro MPD diffractometer (Panalytical, Almelo, The Netherlands) using Cu$K\alpha$ (λ=1.5418 Å) radiation at 40 mA, 40 kV. The step size of 0.03° was used in the scan range 1–40° (2θ). The peak arising from (0 0 3) planes of LDH powder was used to calculate the basal spacing in all the samples using the Bragg's equation. Fourier transform infrared (FTIR) spectra of the as prepared powders were recorded at room temperature using the KBr (Sigma Aldrich, ≥99%) pellet method (sample: KBr=1:100) on a F Varian 3600 (USA) spectrometer in the 400–4000 cm^{-1} range with average of 50 scans. Particle morphology and size of ZnAl-LDH and ZnAl-LDH–MTX samples were examined by transmission electron microscope (TEM) using FEI Tecnai $30G^2$ S-Twin (Netherland) operated at 300 kV and a Carl Zeiss SMT AG SUPRA 35VP (Germany) field emission scanning electron microscope (FESEM). The elemental composition of ZnAl-LDH and ZnAl-LDH–MTX samples was studied using energy dispersive spectroscopy (EDS) attached to the TEM. Particle size of both ZnAl-LDH and ZnAl-LDH–MTX powders was measured by dynamic light scattering technique using a Microtrac Zetatrac, PA (USA) on respective aqueous suspensions. The elemental analyses for carbon, hydrogen and nitrogen (CHN) of ZnAl-LDH–MTX sample was conducted using model-2400, series II CHN analyzer (Perkin Elmer, USA). Thermogravimetric analyses of sample powders were carried out at a heating rate of 10 °C/min in air (thermooxidative analysis) from ambient to 1000 °C using NETZSCH STA 409 CD simultaneous thermal analyzer. HPLC (Shimadzu LC-20AT, Japan) was used to determine the MTX loading and release from ZnAl-LDH nanovehicle in PBS at pH 7.4.

3. Results and discussion

3.1. XRD analysis

The ZnAl-LDH precursor was prepared by coprecipitation of the component hydroxides at constant pH with exchangeable nitrate anions in the gallery space [27]. The precipitate of ZnAl-LDH is formed according to the overall equation:

$$2Zn(NO_3)_2 + Al(NO_3)_3 + 6NaOH \rightarrow [Zn_2Al(OH)_6](NO_3^-) + 6NaNO_3$$

A schematic presentation of the intercalation of MTX in to the LDH interlayers is shown in Scheme 1. The powder XRD patterns of ZnAl-LDH and ZnAl-LDH–MTX are shown in Fig. 1. The pattern for ZnAl-LDH is characteristic of the LDH structure with reasonably well crystallized hydrotalcite-like phase [27,28], exhibiting rather sharp and symmetric 00*l* reflections. The peaks have been

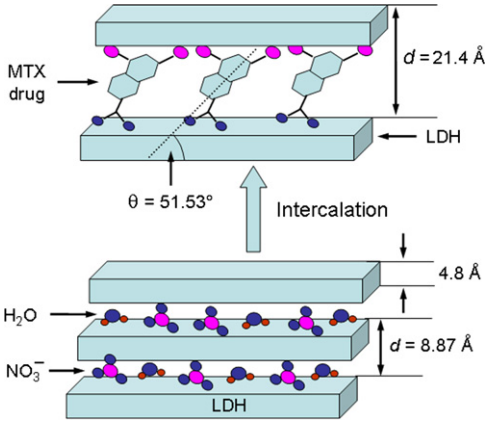

Scheme 1. Schematic diagram showing the intercalation of MTX into the LDH interlayers.

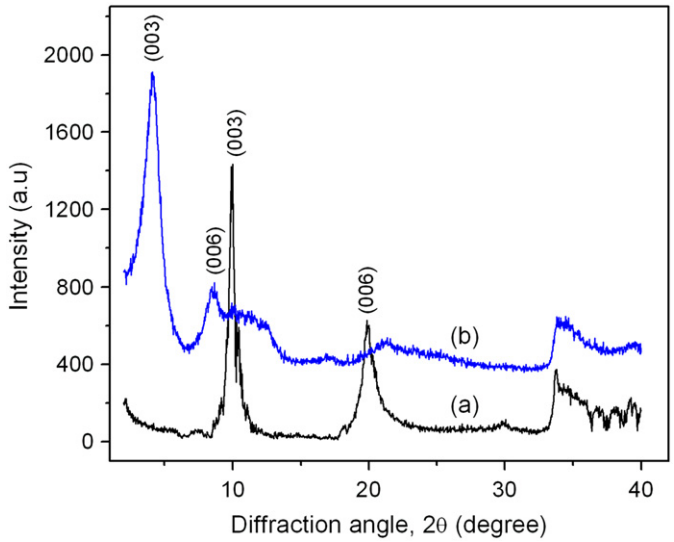

Fig. 1. Powder X-ray diffraction patterns of (a) ZnAl-LDH and (b) ZnAl -LDH–MTX nanopowders.

indexed to a hexagonal lattice with rhombohedral space group [27] with layered features. The basal spacings (d_{003}) is estimated as 8.87 Å from the (0 0 3) diffraction peak. Taking into account the brucite sheet thickness of ZnAl-LDH to be 4.8 Å [27], the gallery height for ZnAl-LDH is 4.07 Å. The intercalation of MTX into the ZnAl-LDH matrix is evidenced by the shift of (0 0 3), (0 0 6) planes to higher *d*-values. The basal spacing (d_{003}) is increased from 8.87 Å in ZnAl-LDH to that 21.4 Å in ZnAl-LDH–MTX hybrid.

The gallery space for ZnAl-LDH–MTX hybrid material is found to be 16.6 Å, which is smaller than the longitudinal molecular length of 21.2 Å for MTX molecule. This is due to a stronger interaction between the anionic carboxylate groups of MTX and cationic brucite layer. Thus the MTX molecule is arranged in a tilted configuration with an angle of tilt of ~51.53° within the brucite layers of LDH (Scheme 1) [29,30].

3.2. TEM analysis

Intercalation of MTX into LDH was also confirmed from TEM micrographs of pristine ZnAl-LDH and ZnAl-LDH–MTX powders shown in Fig. 2. Average interlayer spacing in pristine LDH is estimated as ~8.9 Å from the observed lattice fringes and that increased to 21.3 Å in case of ZnAl-LDH–MTX hybrid, which is very similar to the observations from XRD.

The morphology of the LDH and its intercalated counterpart represent nanofoil-like two-dimensional structures. No significant differences in particle morphology were apparent in any of the ZnAl-LDH and ZnAl-LDH–MTX samples at the magnification used (~200 000) (TEM images shown in Fig. S2 (Supplementary material)). Pristine ZnAl-LDH shows nanofoil-like particle morphology in the size range 100–300 nm.

3.3. FESEM analysis

FESEM micrographs of pristine LDH and ZnAl-LDH–MTX are shown in Fig. 3, which show large clusters of dimension > 500 nm of flaky LDH particles in the pristine sample.

Incorporation of large molecules of MTX into LDH might has resulted in exfoliation of LDH layers [18] resulting in reduction of average size to > 200 nm as was reflected in TEM (Fig. S2b).

The EDS spectra of LDH and LDH–MTX hybrids taken during TEM analyses are shown in Fig. 4 and the data are given in Table 1. It shows that ZnAl-LDH has Zn:Al molar ratio of 1.90:1.00,

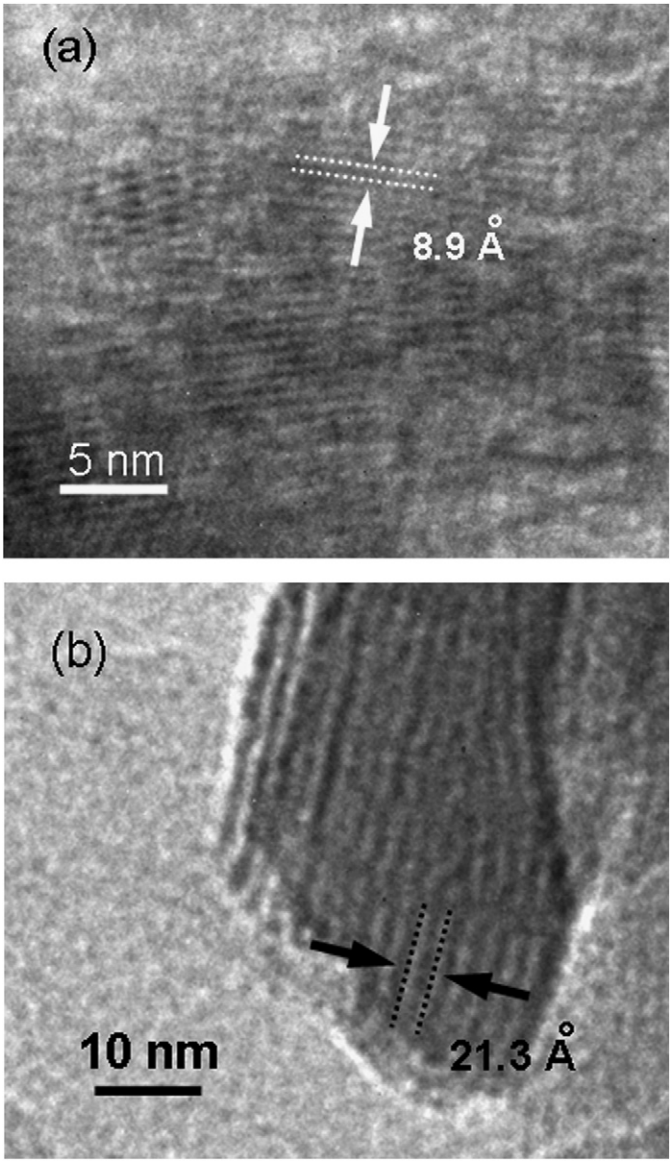

Fig. 2. High-resolution TEM micrographs of (a) pristine ZnAl-LDH and (b) ZnAl-LDH–MTX nanopowders showing layered structure of LDH and intercalated LDH–MTX hybrid.

which is slightly lower than the value of 2:1 used in the starting precursor solution. However, the ratio is close to the that of the precursor solution in ZnAl-LDH–MTX hybrid (1.92:1). The small variation (1%) in the Zn:Al molar ratio between the LDH and LDH–MTX hybrid is due to experimental error and is well within the acceptable limit.

The CHN analyses of Zn-Al-LDH and ZnAl-LDH–MTX are given in Table 2. The amount of MTX intercalated into the interlayer space of ZnAl-LDH was found to be 345.011 mg of MTX/g of LDH–MTX. This corresponds to approximately 34.5 wt% MTX in the LDH–MTX formulation.

3.4. Thermal analysis

Thermogravimetric curves (TG), carried out on LDH, MTX and LDH–MTX under air purge (thermooxidative analysis), are shown in Fig. 5. The ZnAl-LDH powder shows a typical thermogram of hydrated product losing ~32.7% of its mass on heating till 1000 °C. The loss is spread over three major decomposition steps

as evident from the derivative plot of TG. The 1st step at ~115 °C is due to the removal of adsorbed moisture (~5.3%).

The removal of structural water (~17.7%) is spread over the temperature range 210–325 °C. The remaining loss of ~9.3% is attributed to the loss of charge balancing interlayer nitrate ions.

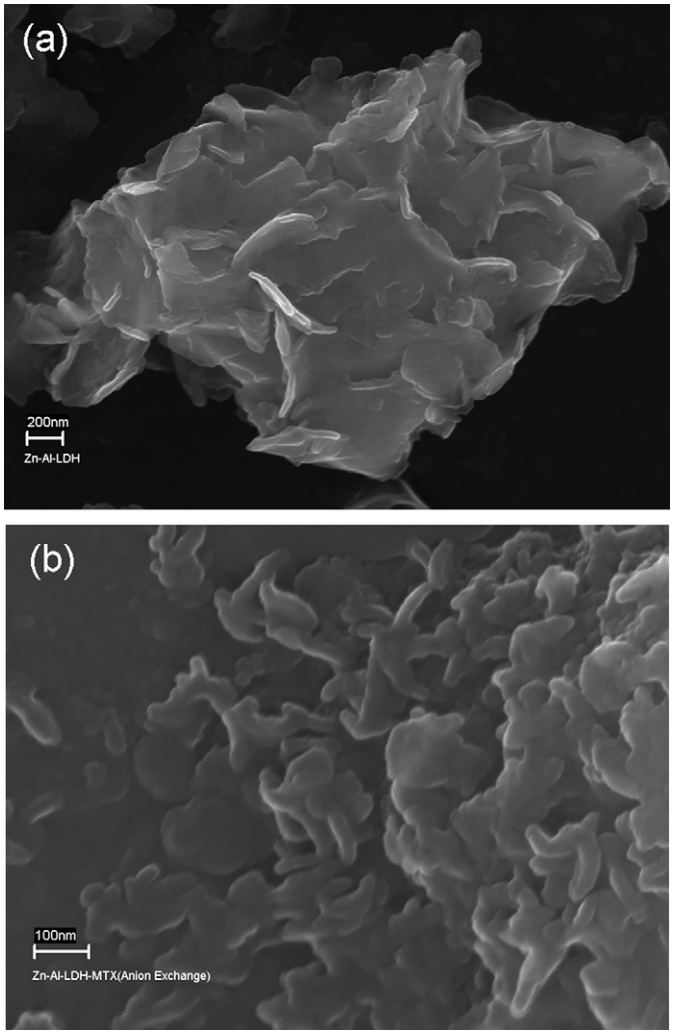

Fig. 3. FESEM micrographs of (a) pristine ZnAl-LDH and (b) ZnAl-LDH–MTX hybrid materials.

Table 1
EDS analysis of ZnAl-LDH and ZnAl-LDH–MTX nanohybrid from FESEM.

Elements	Zn-Al-LDH		ZnAl-LDH–MTX	
	Weight per cent (%)	Atomic per cent (%)	Weight per cent (%)	Atomic per cent (%)
N	2.43	4.67	15.78	26.99
O	38.47	64.07	33.15	49.62
Al	10.78	10.75	8.99	7.98
Zn	48.30	20.50	42.06	15.40

Table 2
CHN analysis of Zn-Al-LDH and ZnAl-LDH–MTX nanohybrid.

Element	Content (%)	
	ZnAl-LDH	ZnAl-LDH–MTX
C	0.41	18.27
H	2.38	3.74
N	4.20	10.02

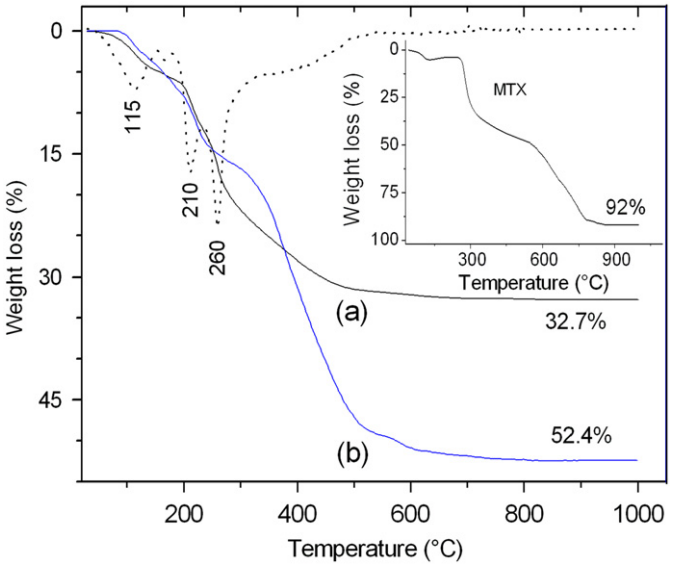

Fig. 5. Thermogravimetry plots of (a) pristine ZnAl-LDH and (b) ZnAl-LDH–MTX hybrid. The thermogram of MTX is shown as inset. The derivative of TG data for LDH is shown as dotted line.

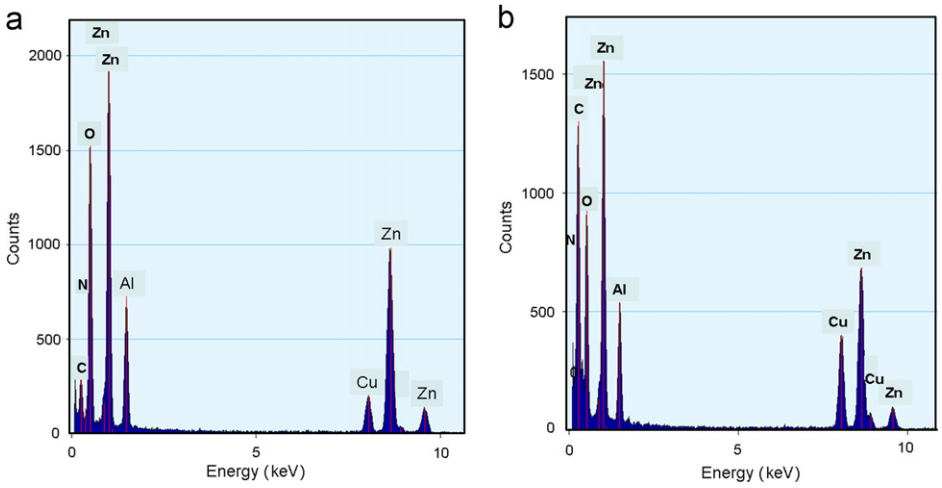

Fig. 4. Energy dispersive spectrum of pristine (a) ZnAl-LDH and (b) ZnAl-LDH–MTX indicating the presence of Zn, Al, O and nitrogen.

The TG pattern for the MTX intercalated hybrid LDH–MTX is quite similar to the same of pristine LDH except that it loses 52.4% mass on heating to 1000 °C. The loss of ~34.1% mass, in the range 320–750 °C is attributed to the intercalated MTX decomposition. The decomposition temperature of unbound MTX ca. 275 °C, as shown in the inset of Fig. 5 is shifted to relatively to higher temperature of ~370 °C in ZnAl-LDH–MTX. This indicates the enhanced thermal stability of MTX due to electrostatic interaction within the layered structure of LDH [18]. Based on thermogravimetric analyses, the loading of MTX in ZnAl-LDH is estimated as 33.22 wt% (Supplementary material). This is in good agreement with the MTX loading estimated from the CHN analysis of ZnAl-LDH–MTX (34.5%) given in Table 2.

3.5. FTIR spectra

The FTIR spectra of pristine LDH, MTX molecule and LDH–MTX hybrids are shown in Fig. 6. Two bands at 600 and 428 cm^{-1} can be attributed to the lattice vibrations of metal–oxygen and metal–hydroxyl bonds. The absorption band at 3438 cm^{-1} signifies the stretching vibration of labile hydroxyl group or physically adsorbed water molecule in ZnAl-LDH [31]. The presence of a strong band at 1384 cm^{-1} signifies the existence of NO_3^- anions in ZnAl-LDH structure [32]. The absence of any band at 1357 cm^{-1} reveals the fact that no CO_3^- anion was present in ZnAl-LDH. The bending vibration of water molecules in ZnAl-LDH was detected at 1609 cm^{-1}. MTX intercalated ZnAl-LDH material showed symmetric and asymmetric stretching vibration of COO^- (νCOO^-) at 1373 and 1554 cm^{-1}, respectively.

The stretching vibrations at 1405 and 1606 cm^{-1} arises due to C=C stretching of MTX. The intensity of nitrate peak in LDH–MTX complex was found to be very low, which signifies that MTX was intercalated into LDH matrix by the exchange of NO_3^- anions. All of these suggest the presence of methotrexate in ZnAl-LDH in the intercalated form.

3.6. Particle size analysis

The hydrodynamic sizes of pristine and methotrexate intercalated ZnAl-LDH in aqueous slurry are measured by light scattering and are given in Fig. 7. The average size of LDH particles in aqueous suspension is 370 nm with polydispersity index (PDI 0.541). It is known that if the size of particles responsible for photon scattering increases by one order of magnitude, the scattered light intensity increases by about a million times [33]. The algorithm in the size measurement software converts the intensity of photon signal to size. The size data of ZnAl-LDH shows (Fig. 7) a bimodal distribution of sizes over ~172 and 710 nm with PDI 0.541, which indicates that the aqueous slurry of ZnAl-LDH contains clusters of ~700 nm size and the majority of the particles in LDH are below 200 nm.

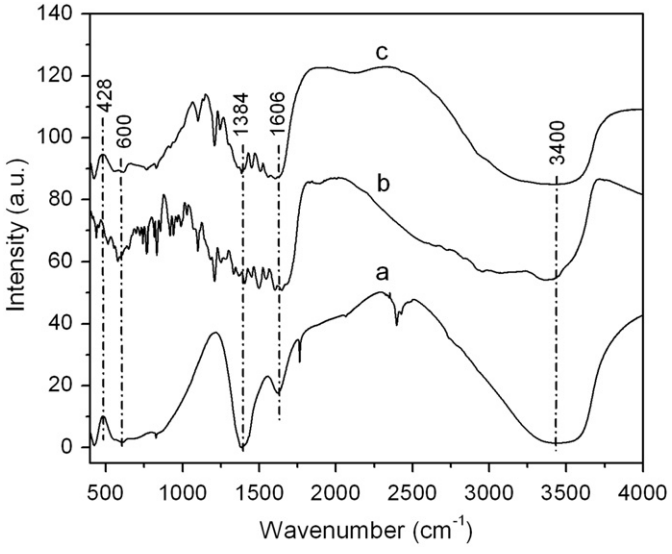

Fig. 6. FTIR spectroscopy of (a) pristine ZnAl-LDH (b) solid MTX, and (c) ZnAl-LDH–MTX nanopowders.

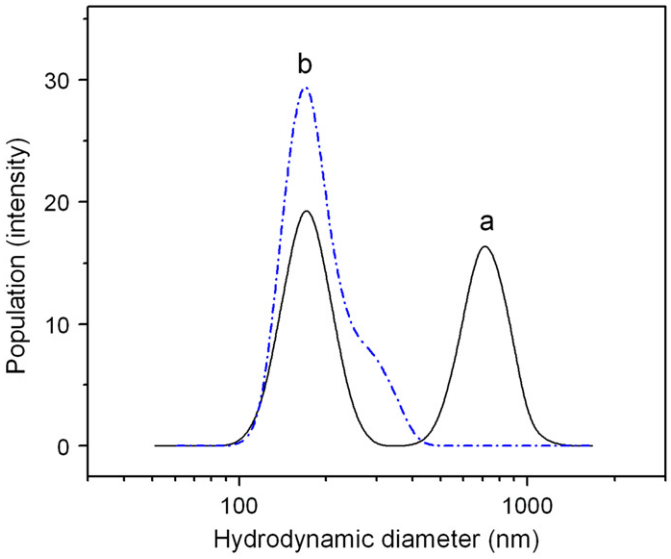

Fig. 7. Particle size distribution (intensity) of (a) ZnAl-LDH and (b) ZnAl-LDH–MTX as measured by light scattering technique.

The hydrodynamic diameters slightly decreased on MTX intercalation to 176 nm (PDI 0.315) as was also observed from TEM (Fig. S2) and FESEM (Fig. 3) observations. The reduction of size on MTX intercalation is due to the exfoliation of the layered LDH structure. The majority of the ZnAl-LDH–MTX nanoparticles have particle sizes below 200 nm, which suggests that most of these nanocarriers can reach the target cells [24] during drug delivery.

3.7. In vitro drug release study

Fig. 8 shows the MTX release profile from the LDH matrix at physiological pH (7.4) at a constant temperature of 37 °C. The release kinetics of MTX following Rigter–Peppas model is shown in the inset. The release of the MTX from LDH–MTX hybrid appears to be complicated and not available in the open literature. The release of the drug up to 10 h appeared to follow a faster kinetics without any burst phenomenon occurring at the beginning of the release tests [34]. This phenomenon may primarily be attributed to the release of MTX molecules from the exposed surfaces followed by subsequent release of MTX anion from the interlayer space of LDH [32]. The later stage of slow release (after 10 h) of MTX is governed mainly by diffusion.

The release profile shows that ~50% of the incorporated MTX was released in 6 h and it increased nonlinearly to ~90% in 24 h. Entire MTX release (~99.9%) within the time frame of 48 h clearly indicates the ability of LDH in controlled drug release. The cumulative release (%) of MTX is nonlinear with time elapsed, and conforms to a power law dependence as given in Eq. (1)

$$R = at^b + ct^d \quad (1)$$

where 'R' is cumulative drug released (%) in time 't' and the constants $a=22.35$, $b=0.512$, $c=-1.336$ and $d=1.349$. Guar gum

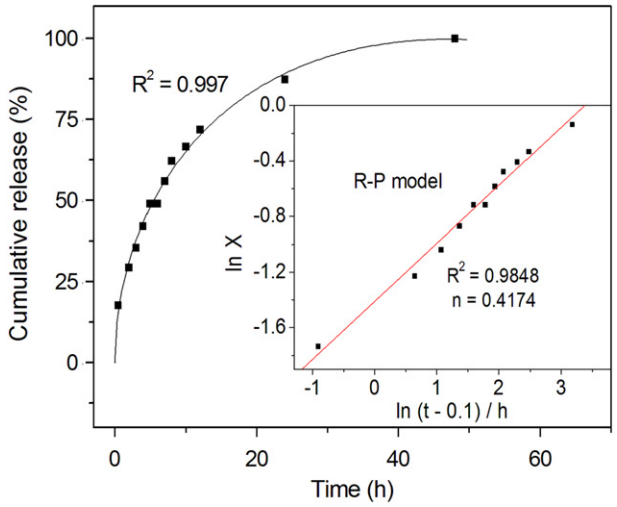

Fig. 8. MTX release profile from ZnAl-LDH–MTX matrix as a function of time. The solid line is a nonlinear fit to the data following Eq. (1). The release kinetics of MTX following Rigter–Peppas model is shown in the inset. The solid line through the scatter plot is linear fit to the data.

Table 3
Drug release kinetic parameters derived from the HPLC analysis of ZnAl-LDH–MTX.

Code	Zero order R^2	First order R^2	Higuchi R^2	Rigter–Peppas model	
				R^2	n
LDH–MTX	0.673	0.9837	0.9704	0.9848	0.417

biopolymer has been shown to exhibit similar behaviour in delivering encapsulated drug payload over time [35]. The MTX release data was fitted to zero-order [36], first-order (Eq. (2) and Fig. S3) [34], Higuchi (Eq. (3) and Fig. S4) [34,36], and Rigter–Peppas (R–P) model (Eq. (4)) [34] to investigate the release dynamics of this system:

$$X = 1 - e^{-k(t-\alpha)} \quad (2)$$

$$X = k(t-\alpha)^{0.5} \quad (3)$$

$$X = k(t-\alpha)^{n} \quad (4)$$

where X, t, k, α and n are the drug release (%), release time, kinetics constant, modified parameter and an exponent respectively. The exponent n, is normally used to describe different release mechanisms. The value of $n < 0.45$ corresponds to the drug diffusion control; $n > 0.89$ is attributed to the dissolution of LDH particles; $0.45 < n < 0.89$ is due to combination of drug diffusion and LDH dissolution in the release process [34].

The fitting results of drug release profiles on the basis of the R–P kinetics model are shown in the inset of Fig. 8. The derived fitting parameters of α, n and R are given in Table 3. It is evident that the MTX drug release from LDH follows Rigter–Peppas model with satisfactory coefficient of 0.9848. This is closely followed by first-order release kinetics (Table 3) with fitting coefficient of 0.9840. The value of n is 0.417 ($n < 0.45$) in R–P model at pH 7.4 indicates that the MTX drug release mechanism is predominantly diffusion controlled [34,36].

4. Conclusions

In this study methotrexate intercalated ZnAl-LDH hybrids have been synthesized using an anion exchange route in the size range of 100–300 nm. Successful intercalation of MTX in the interlayer space of ZnAl-LDH nanopowders was confirmed by XRD, TEM and TG data. Thermooxidative (TG) analysis reveals a shift in decomposition temperature of MTX towards higher temperatures suggesting enhanced stability of MTX in the ZnAl-LDH's cationic framework as a result of successful intercalation of MTX into the LDH gallery. MTX loading in the LDH–MTX formulation was determined to be ~34.50 wt%. Cumulative MTX release from the LDH galleries in PBS (pH 7.4) medium was ~90% in 24 h at 37 °C and the entire drug was released in a period of 48 h. Rigter–Peppas kinetics model provided a good description for the release process demonstrating that drug release was via diffusion. This work provides significant insight into the important area of storage, transport, and delivering of an ionic drug payload over time using ZnAl-LDH as a drug carrier.

Acknowledgments

The authors are grateful to the Director, Central Glass and Ceramic Research Institute, Kolkata, India for providing his permission and facilities to carry on the above work. Thanks are due to all the supporting staffs for various characterization work. Thanks are also due to Dept. of Veterinary Sciences, W. B. University of Animal and Fisheries Sciences for HPLC analysis and IIT, Kharagpur for low angle X-ray diffraction. A special word of acknowledgement to Miss T. S. Sreeremya and M. Soumya, NIIST, CSIR, Trivandrum for their help in the manuscript preparation. This work was supported by the CSIR Network project NWP 0035 (11th 5 year plan).

Appendix A. Supplementary material

Supplementary data associated with this article can be found in the online version at doi:10.1016/j.jssc.2011.07.015.

References

[1] S.J. Palmer, R.L. Frost, T. Nguyen, Coord. Chem. Rev. 253 (2009) 250–267.
[2] L. Feng, X. Duan, Applications of layered double hydroxides. In: Layered Double Hydroxides, 2006, pp. 193–223.
[3] F. Cavani, F. Trifro, A. Vaccari, Catal. Today 11 (1991) 173–301.
[4] F.Z. Zhang, X. Xiang, F. Li, X. Duan, Catal. Surv. Asia 12 (2008) 253–265.
[5] C. Gerardin, D. Kostadinova, B. Coq, D. Tichit, Chem. Mater. 20 (2008) 2086–2094.
[6] M. Chakraborty, S. Dasgupta, S. Sengupta, J. Chakraborty, D. Basu, Trans. Indian Ceram. Soc. 69 (2010) 153–163.
[7] L. Dong, Y. Li, W.G. Hou, S.J. Liu, J. Solid State Chem. 183 (2010) 1811–1816.
[8] A.I. Khan, L.X. Lei, A.J. Norquist, D. O'Hare, Chem. Commun. (2001) 2342–2343.
[9] H. Nakayama, N. Wada, M. Tsuhako, Int. J. Pharm. 269 (2004) 469–478.
[10] S.J. Choi, J.M. Oh, J.H. Choy, J. Phys. Chem. Solids 69 (2008) 1528–1532.
[11] J.H. Choy, Biological Hybrid Materials for Drug Delivery System, Switzerland, 2006, pp. 1–6.
[12] M.A. Xi, M.Z. Liu, H.X. Wang, L. Cai, L. Zhang, C.F. Xie, Q.Q. Li, Cancer 116 (2010) 5479–5486.
[13] N. Jaffe, R. Gorlick, J. Clin. Oncol. 26 (2008) 4365–4366.
[14] J.M. Oh, M. Park, S.T. Kim, J.Y. Jung, Y.G. Kang, J.H. Choy, J. Phys. Chem. Solids 67 (2006) 1024–1027.
[15] S.J. Choi, J.M. Oh, J.H. Choy, J. Nanosci. Nanotechnol. 10 (2010) 2913–2916.
[16] M. Milanesio, E. Conterosito, D. Viterbo, L. Perioli, G. Croce, Cryst. Growth Des. 10 (2010) 4710–4712.
[17] M. del Arco, A. Fernandez, C. Martin, V. Rives, J. Solid State Chem. 183 (2010) 3002–3009.
[18] J.H. Choy, J.S. Jung, J.M. Oh, M. Park, J. Jeong, Y.K. Kang, O.J. Han, Biomaterials 25 (2004) 3059–3064.
[19] L.L. Qin, S.L. Wang, R. Zhang, R.R. Zhu, X.Y. Sun, S.D. Yao, J. Phys. Chem. Solids 69 (2008) 2779–2784.
[20] T. Sliwinski, A. Czechowska, M. Kolodziejczak, J. Jajte, M. Wisniewska-Jarosinska, J. Blasiak, Cell Biol. Int. 33 (2009) 542–547.
[21] R.B. Franklin, L.C. Costello, Arch. Biochem. Biophys. 463 (2007) 211–217.
[22] L.C. Costello, R.B. Franklin, P. Feng, Mitochondrion 5 (2005) 143–153.

[23] B.M. Choudary, B. Kavita, N.S. Chowdari, B. Sreedhar, M.L. Kantam, Catal. Lett. 78 (2002) 373–377.
[24] Z.Z. Chen, E.W. Shi, Y.Q. Zheng, W.J. Li, B. Mao, J.Y. Zhuang, L.A. Tang, J. Am. Ceram. Soc. 88 (2005) 127–133.
[25] N. Yamaguchi, D. Ando, K. Tadanaga, M. Tatsumisago, J. Am. Ceram. Soc. 90 (2007) 1940–1942.
[26] C.X. Liu, W.G. Hou, L.F. Li, Y. Li, S.J. Liu, J. Solid State Chem. 181 (2008) 1792–1797.
[27] S. Gago, T. Costa, J.S. de Melo, I.S. Goncalves, M. Pillinger, J. Mater. Chem. 18 (2008) 894–904.
[28] M.S.S. Roman, M.J. Holgado, C. Jaubertie, V. Rives, Solid State Sci. 10 (2008) 1333–1341.
[29] M. Chakraborty, P. Bose, T. Mandal, B. Datta, T. Das, S. Pal, J. Chakraborty, M. Mitra, D. Basu, Trans. Indian Ceram. Soc. 69 (2010) 229–234.
[30] M. Chakraborty, S. Dasgupta, P. Bose, A. Misra, T.K. Mandal, M. Mitra, J. Chakraborty, D. Basu, J. Phys. Chem. Solids 72 (2011) 779–783.
[31] H. Zhang, S.H. Guo, K. Zou, X. Duan, Mater. Res. Bull. 44 (2009) 1062–1069.
[32] Z.P. Xu, G.Q. Lu, Pure Appl. Chem. 78 (2006) 1771–1779.
[33] Malvern Instruments, 〈http://www.malvern.com/malvern/kbase.nsf/allbyno/KB000792/$file/MRK656-01_An_Introduction_to_DLS.pdf〉 (accessed 1 April 2011).
[34] F.S. Li, L. Jin, J.B. Han, M. Wei, C.J. Li, Ind. Eng. Chem. Res. 48 (2009) 5590–5597.
[35] R.S. Soumya, S. Ghosh, E.T. Abraham, Int. J. Biol. Macromol. 46 (2010) 267–269.
[36] B.S. Dave, A.F. Amin, M.M. Patel, AAPS Pharm. Sci. Tech. 5 (2004).